*Article*

# Tailor-Made Phosphorylated Polyvinyl Alcohol/Tungsten Polyoxometalate Proton Exchange Membrane for a Bio-Electrochemical Energy Storage System

**Vassili Glibin [1], Vahid Vajihinejad [2], Victor Pupkevich [1] and Dimitre G. Karamanev [1,*]**

[1] Department of Chemical and Biochemical Engineering, University of Western Ontario, 1151 Richmond St., London, ON N6A 5B9, Canada; vglibin@uwo.ca (V.G.); vpupkevi@uwo.ca (V.P.)
[2] Department of Chemical and Materials Engineering, University of Alberta, 116k St. and 85 Ave., Edmonton, AB T6G 2R3, Canada; vajihine@ualberta.ca
[*] Correspondence: dkaraman@uwo.ca

**Abstract:** In this work, the synthesis of a phosphorylated polyvinyl alcohol (p-PVA)/polyoxometalate (tungsto-phosphate) membrane for the BioGenerator, a bio-electrochemical energy storage technology, is reported. It was shown that bonding of lacunary tungsto-phosphate ions to the carbon skeleton of a polymer matrix results in an increase in proton conductivity of up to 2.7 times, compared to previously studied phosphorylated PVA membranes. Testing of the membrane in an actual $Fe^{3+}/H_2$ electrochemical cell showed that it performs significantly better ($0.28$ W·cm$^{-2}$ at $0.79$ A·cm$^{-2}$) than the previously used commercial Selemion HSF (Japan) membrane ($0.18$ W·cm$^{-2}$ at $0.60$ A·cm$^{-2}$).

**Keywords:** proton exchange membrane; energy storage; bio-electrochemical system; lacunary tungsto-phosphate

## 1. Introduction

The transition from a fossil-fuel-driven economy to one based on clean renewable energy is one of the main problems that our society currently faces. One of the major challenges of the wide implementation of renewables, mainly wind and solar, is their grid integration. It is well known that the time profiles of wind and solar power generation, which widely vary in time, do not fit the power consumption profile. One of the most promising solutions to the problem of variability of renewable power is energy storage, which was recently dubbed "the Holy Grail" of the renewable energy [1]. The main idea of energy storage is to convert electrical energy, which is not directly storable, into another, storable form of energy. After storing the latter, it can be converted back to electricity, thus smoothing the variable electrical input. There are many energy storage technologies under development, based in general on physical and/or chemical principles. Among the most promising storable forms of energy is the energy of hydrogen. In hydrogen-based energy storage, there are three main elements: (i) conversion of the excess of electricity to hydrogen by electrolysis; (ii) storage of the produced hydrogen; (iii) conversion of the stored hydrogen back to electricity (re-electrification). The processes of electrolysis and hydrogen storage are relatively well developed. However, the conversion of hydrogen to electricity is still under development. Fuel cells are the main candidates for that conversion.

Both the anodic and cathodic reactions in conventional fuel cells are purely electrochemical reactions. However, recently microbial fuel cells were introduced, in which the anodic and/or cathodic reactions are catalyzed by microorganisms [1]. We have recently proposed a novel, fuel cell-based bio-electrochemical system for such energy conversion, named BioGenerator [2,3], where the chemolithoautotrphs *Leptospirillum ferriphilum* oxidize

biologically ferrous to ferric ions, using the energy of atmospheric oxygen reduction in the process of microbial respiration:

$$2FeSO_4 + \tfrac{1}{2} O_2 + H_2SO_4 = Fe_2(SO_4)_3 + H_2O \tag{1}$$

The $Fe^{3+}$ is then used as an electron acceptor (oxidant) at the cathode of an electrochemical cell:

$$Fe^{3+} + e^- = Fe^{2+} \tag{2}$$

where the electron donor (fuel) at the anode is hydrogen:

$$H_2 = 2H^+ + 2e^- \tag{3}$$

The schematics of the BioGenerator is shown in Figure 1. It should be noted that while the anolyte is a gas (hydrogen), the catholyte is a liquid (an aqueous solution of mostly ferric sulfate and sulfuric acid).
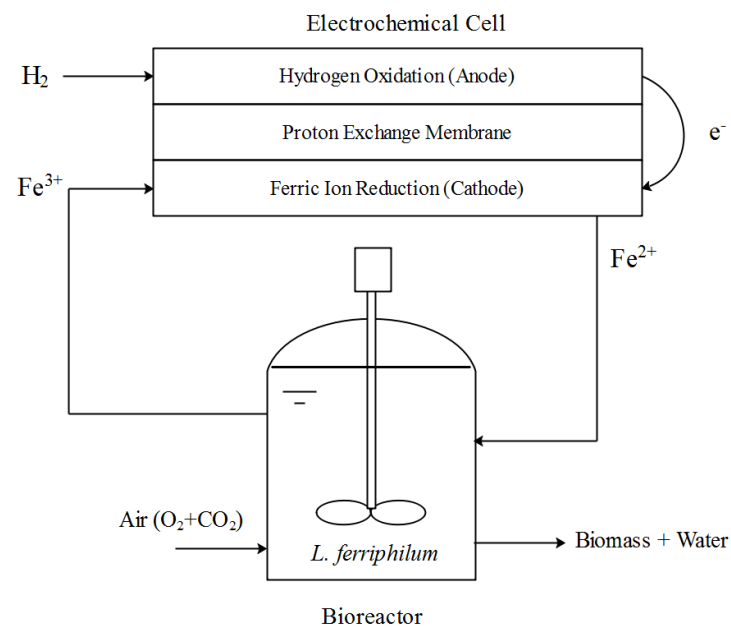


**Figure 1.** Schematics of the BioGenerator.

The BioGenerator fits perfectly the definition of a biological, and more specifically, microbial, fuel cell (MFC) [1]. However, there is one significant difference between the vast majority of known MFCs and the BioGenerator, i.e., while the main goal of most other MFCs is to utilize non-conventional fuels such as sugars, wastewater and sediments by using a biological component at the anode [2,3], the goal of the BioGenerator was to solve the main problems of conventional fuel cells by using a biologically-based cathode, as well as hydrogen as a fuel source at the anode and, as a result, to develop a commercially viable microbial fuel cell.

The anodic and cathodic compartments of the electrochemical cell are separated by a proton exchange membrane; the latter is one of the key components of the entire BioGenerator. The membrane needs to meet a number of requirements, such as mechanical strength, high proton conductivity, low ferric ions diffusivity, long-term chemical stability and low cost. It was already found experimentally that most popular commercially available ion-exchange membranes (Nafion-117, Nafion-115, Nafion-112, Neosepta CMS, bipolar Selemion HSF) do not satisfy a number of the above-mentioned requirements [4,5]. Among them, the bipolar Selemion HSF membrane showed the best performance [4], but was still far from ideal. Several attempts were made in our laboratory to develop membranes that could meet most of the above-mentioned requirements [5–8]. In particular, the testing of

the partially phosphorylated polyvinyl alcohol (p-PVA) membrane in a single $Fe^{3+}/H_2$ redox fuel cell showed performance comparable to Selemion HSF membrane in the region of medium current densities (up to 150 mA/cm$^2$) [7]. The intrinsic proton conductivity of the non-modified PVA membrane was found to be up to $5.5 \times 10^{-3}$ S/cm at 22 °C. According to the literature [9–20], to increase the proton conductivity of polyvinyl alcohol based membranes, it was proposed to use different organic and inorganic modifiers such as phosphonic acid functionalized aminopropyl triethoxysilane [9], sulfonic acids [10,11], phosphonic acids [12,13], combination of boric acid and boron phosphate [14], heteropoly-acids (HPAs) [15–20] and others. Heteropolyacids (polyoxometalates) are considered to be among the most attractive inorganic modifiers of polymer membranes due to their high proton conductivity [21]. Among different types of HPAs, the Keggin-type heteropolyacids are quite well studied [22]. The basic structural unit of these HPAs is the Keggin anion $[X^{n+}M_{12}O_{40}]^{(8-n)-}$, which consists of a central tetrahedron (X = $Si^{4+}$, $B^{3+}$, $P^{5+}$ and other nonmetals), surrounded by twelve edge-shared $MO_6$ octahedron (M = $Mo^{6+}$, $W^{6+}$) [22]. The high acidity of Keggin-type HPAs is caused by the distribution of the negative charges between many atoms of the polyanions, which results in low attraction of protons to anions. The main disadvantage of HPAs as modifiers is their high solubility in water. To overcome this problem, three different approaches have been proposed: (i) embedding of HPAs into $SiO_2$/polymeric matrix [17]; (ii) covalent bonding to oxide nanoparticles which can further be embedded physically in a polymeric matrix [18–20]; (iii) covalent bonding of lacunary 11-silicotungstic acid (HSiW11) to phenol phosphonate ester sidechains of a fluoroelastomer [23]. It is well known that lacunar tungstophosphate anions are formed from the parent $[PW_{12}O_{40}]^{3-}$ anion during alkalization of the $H_3PW_{12}O_{40}$ acid [23]. The $[PW_{12}O_{40}]^{3-}$ anion is stable at pH < 2, above which the mono-vacant $[PW_{11}O_{39}]^{7-}$ anion is formed, converting to the tri-vacant $[PW_9O_{34}]^{9-}$ anion at pH > 7. Particularly, the lacunar tri-vacant $[PW_9O_{34}]^{9-}$ with organohalogenosilanes $SiRX_3$ (R = $C_2H_5$, CH=$CH_2$, Phenyl, N(C(CH$_2$)$_3$) [24], organo-phosphonic acids [25] and other electrophilic compounds resulting in the formation of organic–inorganic hybrid materials.

Based on the above literature survey, it can be seen that the use of lacunar tungsto-phosphate anions, as modifiers for PVA based membranes, have not been studied so far.

The purpose of this work was to synthesize a cation exchange membrane for application in a $Fe^{3+}/H_2$ redox cell, which is at the heart of a novel bio-electrochemical system for energy storage. A hybrid p-PVA (partially phosphorylated polyvinyl alcohol)/tungsto-phosphate membrane was synthesized through the reaction between phosphonic groups of the phosphorylated PVA-matrix and lacunar tungsto-phosphate anions. They were formed in situ during the acidification of the impregnated p-PVA films with the solution containing sodium tungstate, $H_3PW_{12}O_{40}$ and hydrogen peroxide. The main physico-chemical properties of the membrane were determined.

## 2. Materials and Methods

### 2.1. Chemicals

For preparation of the membrane, the following analytical grade reagents were used: polyvinyl alcohol (Elvanol 71-30, DuPont, Berlin, Germany), hypophosphoric acid, $H_3PO_2$ (Sigma-Aldrich, St. Louis, MO, USA), the phosphotungstic acid, $H_3PW_{12}O_{40} \cdot 29H_2O$ (Caledon Laboratories, Mississauga, Canada), sodium tungstate, $Na_2WO_4 \cdot 2H_2O$, (Sigma-Aldrich, St. Louis, MO, USA), nitrilo-tris(methylene) triphosphonic acid, $N[CH_2PO(OH)_2]_3$ (Sigma-Aldrich, St. Louis, MO, USA), and 30% solution of hydrogen peroxide (Caledon Laboratories, Mississauga, Canada).

### 2.2. Membrane Preparation

The preparation of the membrane involved several steps. The first step consisted of the phosphorylation of a polyvinyl alcohol. For this purpose, pre-determined quantities of $H_3PO_2$ and nitrilo tris(methylene) triphosphonic acid, $N[CH_2PO(OH)_2]_3$ were added

to 100 mL of 7% wt. aqueous solution of polyvinyl alcohol to obtain a solution with the following weight ratios (in %): 70 PVA/15 $H_3PO_2$/15 $N[CH_2PO(OH)_2]_3$. The solution was stirred mechanically and heated slowly to reach a temperature of 95 °C. Further, the solution was casted in three polymer Petri dishes (78 mm in diameter) and kept for 3 days at room temperature for the films to form. The obtained films were thermally treated in an oven at 120 °C to form the phosphonic acid functional groups and to perform the crosslinking of PVA with $N[CH_2PO(OH)_2]_3$ through esterification of OH$^-$ groups of PVA [7,26]. This process took approximately 1.5 h to achieve a desired extent of cross-linking. The reactions, during the thermal treatment, can be described as follows:

(a) partial dehydration of PVA catalyzed by $N[CH_2PO(OH)_2]_3$ acid, (the strong acids catalyze this process [27])

$$- (CH_2\text{-}CHOH)_n - \overset{-H_2O}{\rightarrow} -(CH_2\text{-}CHOH)_{n-m}\text{-}(CH=CH)_m - \tag{4}$$

(b) partial phosphorylation of the dehydrated PVA with $H_3PO_2$ [7]

$$\begin{aligned} -(CH_2\text{-}CHOH)_{n-m}\text{-}(CH=CH)_m - +k\ H_3PO_2\ +\ 0.5k\ O_{2\,(air)} = \\ -(CH_2\text{-}CHOH)_{n-m}\text{-}(CH=CH)_{m-k}\text{-}(CH\text{-}CH_2\text{-}PO(OH)_2)_k - \end{aligned} \tag{5}$$
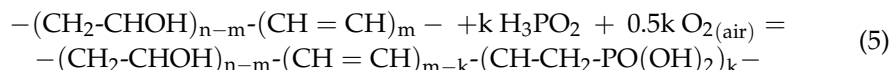
(c) the crosslinking of polymer molecules via esterification of the OH-groups of PVA [7,26].

Further, the films were swollen in 0.5 L of deionized water for 10–12 h, removed, rinsed by de-ionized water and immersed in 100 mL of aqueous solution containing 5.3 g of $Na_2WO_4 \cdot 2H_2O$, 7.5 g of $H_3PW_{12}O_{40} \cdot 29H_2O$, and 5 mL of 30% hydrogen peroxide for 1 h. Then, the films were taken out of the solution and placed in 100 mL of 0.5 M sulfuric acid for 0.5 h to complete the process of the membrane formation. During the process, the films color changed from transparent to light green-yellow. Finally, the films were washed with de-ionized water and stored in 0.005 M sulfuric acid solution.

*2.3. Measurements*

2.3.1. Water Uptake and Linear Swelling Ratio

The film specimens (4 cm × 4 cm) were cut and dried at a temperature of 22 °C until reaching a constant weight ($W_1$). Then they were immersed into 50 mL of de-ionized water at 22 °C for 24 h. Further, the specimens were removed from water and the surface water was carefully removed using a paper tissue. After that, in a timely manner, the specimens were weighed again ($W_2$) and the water uptake ($WU$) was calculated using the following equation:

$$WU(\%) = [(W_2 - W_1)/W_2] \times 100 \tag{6}$$

The dimensional change in the membrane due to water swelling was measured using a ruler or digital micrometer (for the thickness). The dimensional change was calculated as follows:

$$\left(\frac{\Delta D}{D_{dry}}\right)\% = \frac{D_{sw} - D_{dry}}{D_{dry}} \times 100 \tag{7}$$

where $D_{sw}$ and $D_{dry}$ are the dimensions in swollen and dry states, respectively.

2.3.2. X-ray Photoelectron Spectroscopy (XPS)

The XPS study of membrane specimens was performed using a Kratos AXIS Ultra Spectrometer (Shimadzu, Guelph, ON, Canada).

2.3.3. Infrared Spectroscopy

The IR spectrum of the membrane was determined using Nicolet 6700 FT-IR spectrometer (Thermo Scientific, Waltham, MA, USA).

### 2.3.4. Proton Conductivity

The proton conductivity of the synthesized membrane was measured by a direct current two-point-probe method using the setup shown in Figure 2. The measuring cell consisted of four separate compartments. The electrodes in the auxiliary compartments were used to apply an electric potential. The central membrane was the membrane under study (Figure 2), while the other two membranes at the ends of the measuring cell (at the interface of cathode and anode, respectively) were auxiliary cation exchange Nafion 117® (DuPont, Wilmington, DE, USA) and anion exchange Excellion I-200 (SnowPure, San Clemente, CA, USA) membranes.
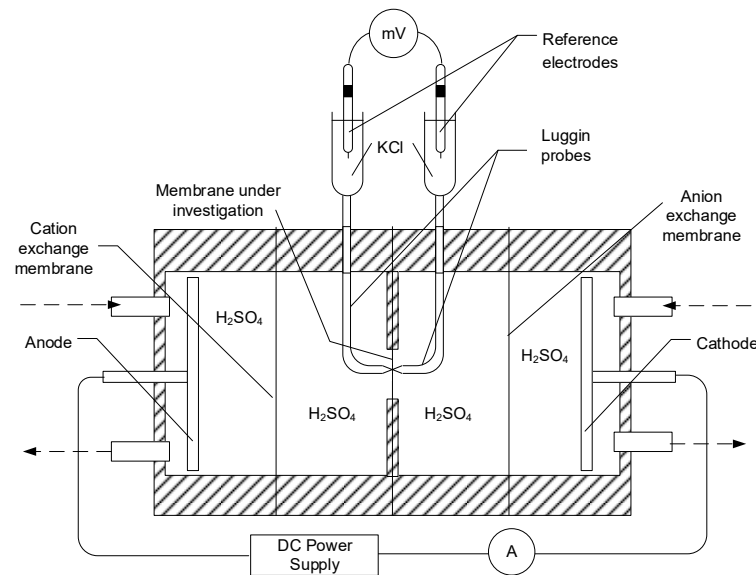


**Figure 2.** Schematic of the apparatus for measuring proton conductivity of membranes. Adapted from [26].

The voltage drop, V (mV), across the membrane was measured by a pair of Luggin capillaries which were filled with saturated aqueous solution of potassium chloride ($KCl_{sat}$) and each of them was connected to a test tube with $KCl_{sat}$, having Ag/AgCl, $KCl_{sat}$ reference electrode in it. The reference electrodes were connected to a pH-meter/mV-meter Orion 420A (VWR, Canada) to measure the potential difference. A 10% $H_2SO_4$ solution was circulated through the auxiliary compartments with a flow rate of 25 mL min$^{-1}$. The voltage drop across the studied membrane was measured as a function of the current density, $i$ (mA·cm$^{-2}$), in the range of 0–90 mA·cm$^{-2}$, while stepwise increasing the electrical current. The area resistance, $R$ ($\Omega^{-1}$ cm$^{2-}$) of the membrane was determined as a slope of the linear part of $\Delta V$–$i$ plot. The conductivity values, $\sigma$ ($\Omega^{-1}$ cm$^{-1}$) were calculated as follows:

$$\sigma = \delta/R \tag{8}$$

where $\delta$ is the membrane thickness (cm).

### 2.3.5. Testing of the Membrane in a BioGenerator $Fe^{3+}/H_2$ Electrochemical Cell

To test the membrane performance in a complete electrochemical cell and to compare its performance with the commercial Selemion HSF membrane, the polarization curves and electrode potentials were obtained using the setup shown in Figure 3.
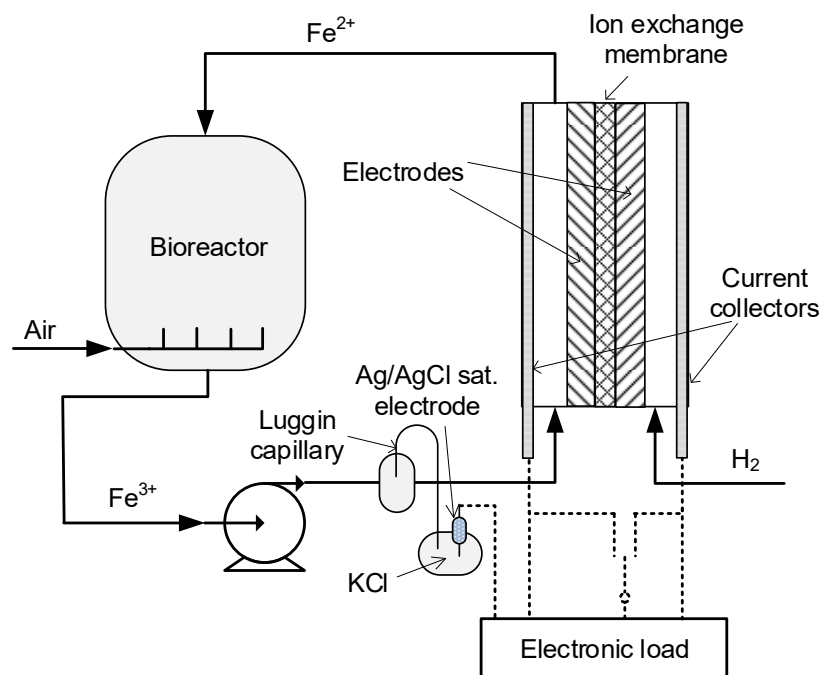
**Figure 3.** Setup for the testing of membranes in the $Fe^{3+}/H_2$ electrochemical cell with microbiological regeneration of $Fe^{2+}$ ions. Adapted from [26].

To measure the potential of the cathode, the reference electrode was connected to a current collector from the cathodic side of the cell via electronic load CHROMA 6314 (Chroma Systems Solutions, Foothill Ranch, CA, USA) and the electrical potential was recorded. The hydrogen pressure in the anodic compartment was kept constant at 35 kPa (gauge) through a controlled supply of pure hydrogen at a flow rate of 15 L min$^{-1}$. Commercially available hydrogen electrode GDE LT 250EWSI (BASF, Fuel Cell, Inc., Somerset, KY, USA) was used as the anode. Activated graphite felt [26] based on Sigratherm felt (SGL, Wackersdorf, Germany) was used as the cathode. Both electrodes had geometric area of 5.3 cm$^2$. The catholyte, 0.45 M $Fe_2(SO_4)_3$ with a pH of 0.8 was pumped from the bioreactor through the cathode in a direction parallel to the membrane with a flow rate of 70 mL min$^{-1}$. The detailed measurement technique was described earlier [26].

## 3. Results and Discussion

### 3.1. Basic Physico-Chemical Properties

The fabricated membranes had a light green-yellowish color and were brittle when dry. On the contrary, in a swollen state they were quite flexible and mechanically robust to be used and tested in an electrochemical cell. Apparently, the high flexibility of membranes can be explained by the plasticizing properties of the absorbed water. The thickness of all the obtained membranes was measured to be $0.015 \pm 0.005$ mm. The water uptake and the dimensional changes (changes in the length and thickness) of the membranes of different composition were observed to be similar, and were 40% and 33%, respectively. The membranes were chemically stable in diluted solutions of strong inorganic acids. This was determined qualitatively by the absence of the blue coloration of the de-ionized water and 10% $H_2SO_4$ solution (which were in contact with the membrane for one week at 22 °C) after addition of a few drops of 5% solution of $TiCl_3$.

### 3.2. XPS Study

The results of the XPS study are shown in Figures 4 and 5. In Figure 4, the peaks of the deconvoluted XPS spectrum are referred to the binding energies of $C_{1s/4}$ carbon, which correspond to the C-C carbon chain with C-H bonds (284.8 eV) and to the different oxygenated functionality of the C-C skeleton (C-OH bonds at 286.3, C=O bonds at 287.8

and CO(OH) groups at 289.1 eV). It can also be seen from Figure 4 that the organic matrix of the membrane includes about 23% of different oxygen-containing functional groups.
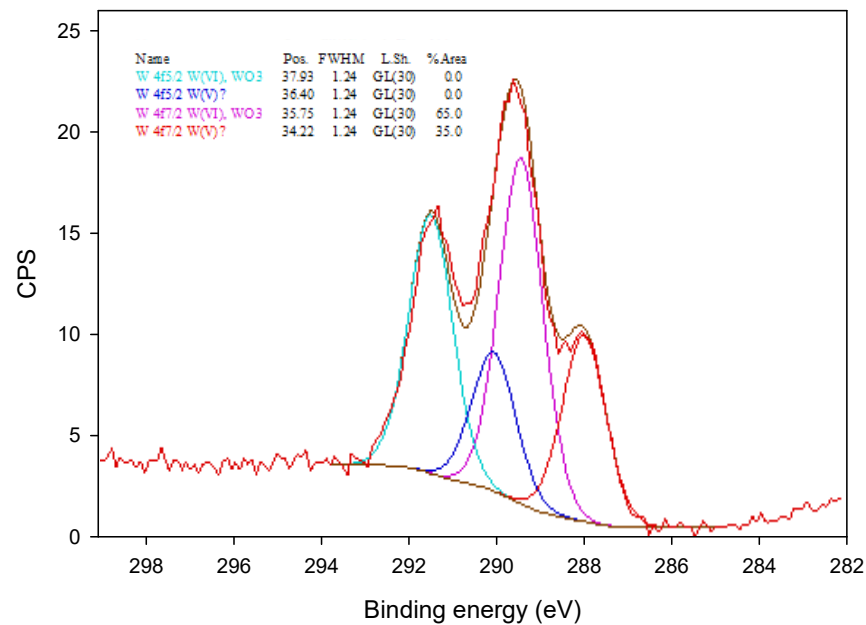


**Figure 4.** The XPS spectrum of organic network of the membrane.
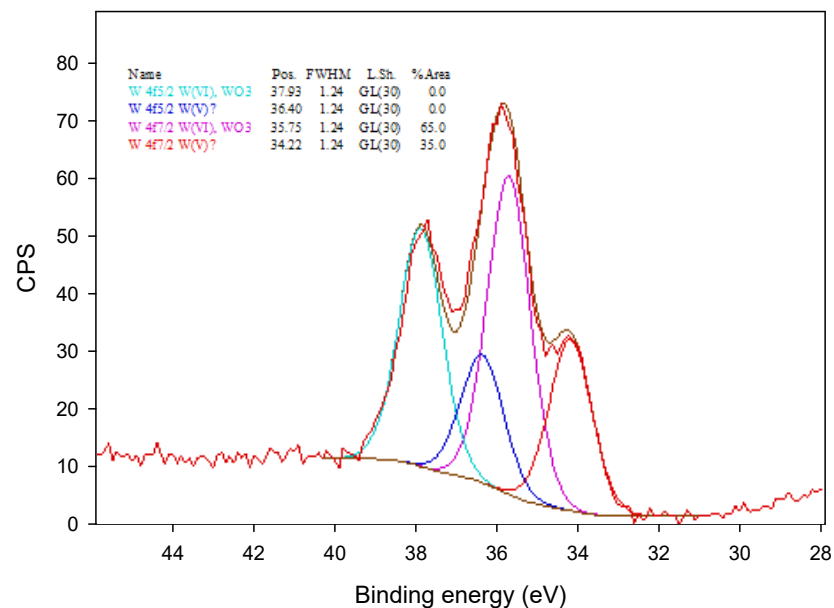


**Figure 5.** The XPS spectrum of the tungsto-phosphate membrane.

In Figure 5, the $W_{4f}$ XPS spectrum was fitted with two different doublets of $W_{4f(5/2)}$ and $W_{4f(7/2)}$ located at 37.93 and 36.40, and 35.75 and 34.22 eV, respectively. The peaks at 37.93 and 35.75 eV correspond to the W(VI) oxidation state, and the peaks at 35.75 and 34.22 eV were assigned to the partially reduced oxidation state, W(V), of tungsten [28]. The appearance of partially reduced oxidation state of tungsten is presumably a result of the incorporation of tungsten oxometallate ions into the polymer matrix.

### 3.3. IR Spectroscopic Study

Vibrational spectroscopy gives useful information on the structure of membranes. Figure 6 displays the FTIR spectrum of a membrane in the range of wavenumbers between 4000 and 500 cm$^{-1}$. The band positions and their types are summarized in Table 1.
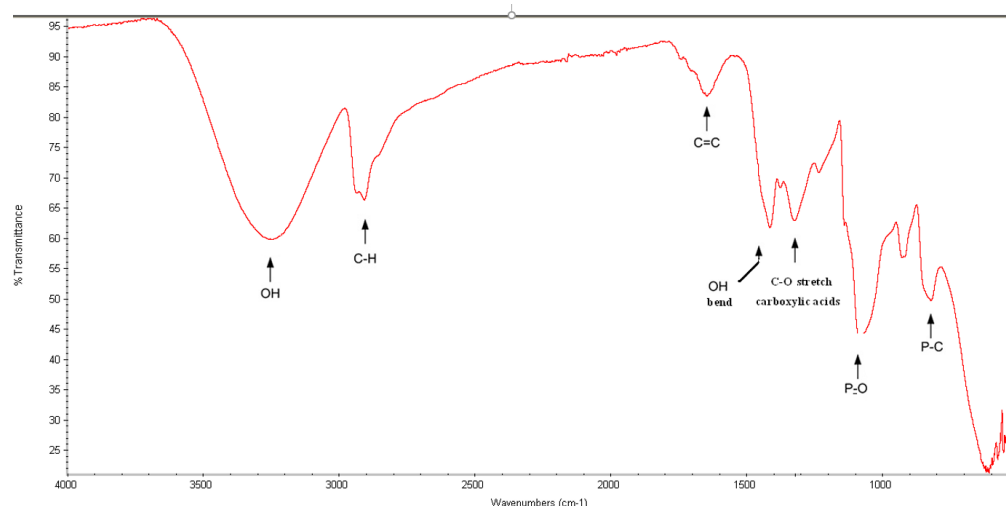


**Figure 6.** The IR spectrum of the membrane.

Alkyl chain vibrations are observed at 2937 and 2903 cm$^{-1}$ (asymmetrical and symmetrical C-H bond valence vibrations), and 1424, (caused by coupling of the O-H scissoring with the C-H wagging in the -CH-OH groups of PVA [29]). The very weak band at 1743 cm$^{-1}$ is probably due to the stretching of C=O bonds from acetate groups remaining in PVA (incomplete hydrolysis of the polyvinyl acetate during PVA synthesis). The bands at 1382 and 1326 cm$^{-1}$ can be attributed to stretching vibrations of C-N bonds in aminophosphonic acids [30] and free P=O bonds [7,31], respectively. The band at 1082 cm$^{-1}$ is assigned to the $\nu_{as}$(P-O) stretching modes of the central PO$_4$ tetrahedron in [PW$_9$O$_{34}$]$^{9-}$ anion [25]. The shoulder at ~1000 cm$^{-1}$ is referred to $\nu_{as}$(P-O) stretching mode in a phosphonic acid [25] and/or $\nu$(C-O(P)) bridge in phosphate esters [7,32]. Some frequencies of relevance, namely, the bands at 931 cm$^{-1}$ ($\nu_{as}$(W=O$_t$ stretching mode, subscript represent the terminal oxygen) and 829 cm$^{-1}$ ($\nu_{as}$(W-O-W)) belong to this anion, and the band at 603 cm$^{-1}$ is referred to the bending vibrations of O-P-O linkages in the phosphonic acid derivates of [PW$_9$O$_{34}$]$^{9-}$ anion [25]. The weak band at 1708 cm$^{-1}$ reveals the presence of the isolated H$_3$O$^+$ ions which are the reason for the high proton conductivity of heteropolyacids [33].

The broad band at 3243 cm$^{-1}$ can be assigned to the OH stretching vibrations of hydrogen bonded OH-groups of phosphonic acids and H$_3$O$^+$ ion [30–33]. On the one hand, the presence of vibrations of W=O and W-O-W bonds belonging to the free [PW$_9$O$_{34}$]-grouping (in organophosphoryl derivates of tri-vacant tungsto-phosphates, these vibrations are shifted to the region of higher wave numbers [25]) indicates their direct bonding to PVA backbone via C-O-W bridges formation; on the other hand, the strong asymmetric bending O-P-O vibrations, which are characteristic for organophosphoryl derivates of [PW$_9$O$_{34}$]$^{9-}$ anion [25], indicate on the similar derivate formation.

**Table 1.** Wavenumbers ($cm^{-1}$), relative intensities and the assignment for IR-bands of the membrane.

| Wave Number | Description | Assignment | Wave Number | Description | Assignment |
|---|---|---|---|---|---|
| 3243 | strong and broad | $\nu$(O-H) groups of phosphonic acids | 1326 | strong | $\nu_{as}$(P=O, free) [8,32] |
| 2937 | strong | $\nu(CH_2)$ [30] | 1222 | medium | $\nu$(P=O, hydrogen bonded) [31] |
| 2903 | strong | $\nu(CH_2)$ [30] | 1137 | shoulder, medium | $\nu$(C-OH) in PVA |
| 1743 | very weak | $\nu$(C=O) of esters [31] | 1082 | strong | $\nu$(P-O) of $PO_4$ tetrahedron [25] |
| 1708 | weak | $\nu(H_3O^+$, free) [32] | ~1000 | shoulder, medium | $\nu_{as}$(P-O) in phosphonic acids [25] or $\nu$(C-O(P)) [7,33] |
| 1646 | medium | $\nu$(C=C) [31] | 931 | medium | $\nu_{as}$(W=O) of $[PW_9O_{34}]^{9-}$ anion [25] |
| 1424 | strong | $\delta$(C-H) of -$CH_2OH$ group of PVA [29] | 829 | medium | $\nu_{as}$(W-O-W) of $[PW_9O_{34}]^{9-}$ anion [25] |
| 1382 | medium | $\nu_{as}$(C-N) [29] | 603 | strong | $\delta_{as}$(O-P-O) [a] [25] |

$\nu$: stretching vibration; $\delta$: bending vibration; as: asymmetric. [a] [PW9O34(RPO(OH)2]5- complex.

Thus, based on the results of the spectroscopic studies (XPS and FTIR), we can assume the occurrence of two reactions leading to the covalent bonding of tungsto-phosphate anions to the polymer matrix. The first one may be presented by the following equations:

(a) epoxidation of the C=C double bonds with $H_2O_2$ (this reaction is catalyzed by aminophosphonic acids [34]):

$$–(CH_2\text{-}CHOH)_{n\text{-}m}\text{-}(CH\text{=}CH)_{m\text{-}k}\text{-}(CH\text{-}CH_2\text{-}PO(OH)_2)_k– \ + \ m\text{-}k\ H_2O_2 \ \rightarrow$$

$$–(CH_2\text{-}CHOH)_{n\text{-}m}\text{-}(\overset{\displaystyle O}{HC\!-\!\!-\!\!-\!CH})_{m\text{-}k}\text{-}(CH\text{-}CH_2\text{-}PO(OH)_2)_k– \ + \ m\text{-}k\ H_2O \tag{9}$$
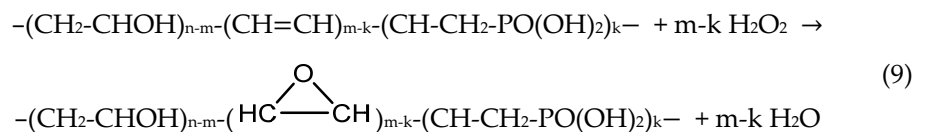
In this reaction, the role of a catalyst is played by the $N[CH_2PO(OH)_2]_3$ acid.

(b) the opening epoxy rings leads to covalent bonding of the lacunar tungsto-phosphate anions, as nucleophiles, to the p-PVA polymer (C-O-W bonds formation). It should be mentioned that the opening of epoxy rings under acidic conditions occurs in two stages: first, the epoxy group gets protonated and, second, the nucleophile attacks the most substituted position in the molecule, which results in the two groups (nucleophile and OH-group) being trans-oriented with respect to each other [35].

Another path is through the reaction between tri-vacant $[PW_9O_{34}]^{9-}$ anion and the accessible -$PO(OH)_2$ functional groups either nitrilo-tris(methylene) triphosphonic acid, $N[CH_2PO(OH)_2]_3$, or -(-CH(OH)-$CH_2$-PO(OH)_2)_k—grouping of the p-PVA or both. These reactions were described, in general, earlier [25]:

$$[PW_9O_{34}]^{9-} + 2RPO(OH)_2 + 4H^+ \ \rightarrow \ \left[PW_9O_{34}(RPO(OH)_2\right]^{5-} + 4H_2O \tag{10}$$
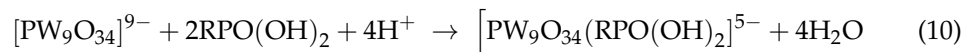
where R is an organic radical.

The comparison between the main parameters of the membrane developed in this work and two commercial membranes is shown in Table 2. It can be seen that, in general, the new membrane has better performance than Nafion 117 and is comparable to Selemion.

**Table 2.** Comparison of the performance of different membranes.

| Membrane | $H^+$ Resistance | Selectivity | Poisoning by $Fe^{3+}$ |
|---|---|---|---|
| Nafion 117 | 0.86 | Intermediate | Yes |
| Selemion HSF | 0.49 | High | No |
| This work | 0.52 | High | No |

### 3.4. Proton Conductivity

The relationships between the voltage drop and current density for p-PVA/tungsto-phosphate membrane and, for a comparison, Nafion-117 and Selemion HSF membranes in 10% $H_2SO_4$ at 22 °C are shown in Figure 7.
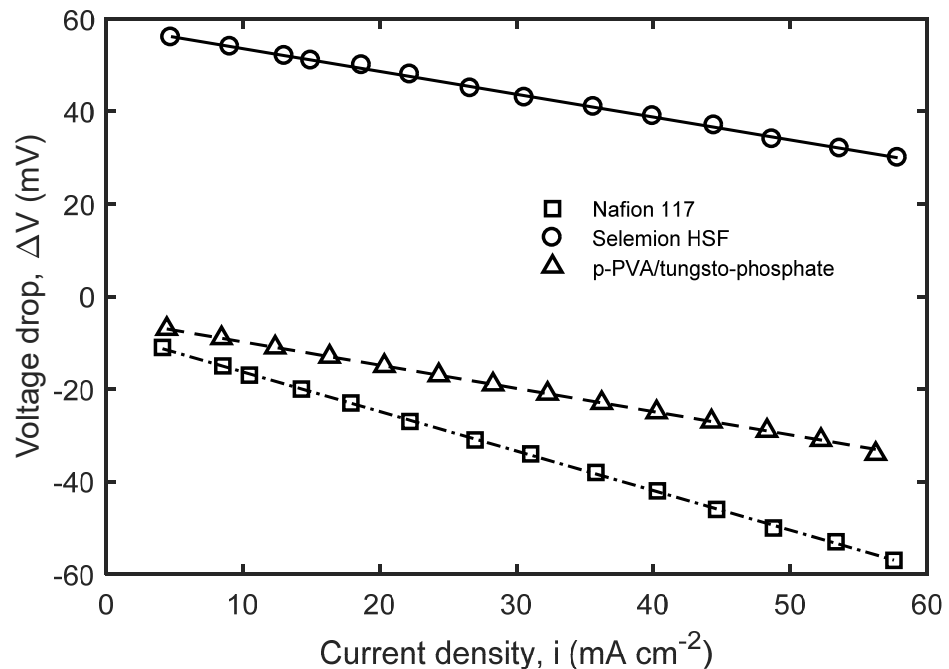


**Figure 7.** Voltage drop as a function of current density for different membranes used in this study.

Prior to taking measurements, the membranes were conditioned in 10% $H_2SO_4$ for 2 h. The values of thickness of p-PVA/tungsto-phosphate, Nafion-117 and Selemion HSF membranes in swollen state were equal to 0.025, 0.025 and 0.020 cm, respectively. It should be noted that the transport of ferric ions through the membranes was insignificant due to the high permselectivity between the ions of $H^+$ and $Fe^{3+}$. As can be seen in Figure 7, the voltage drop dependences for the studied membranes with respect to the current density are represented by mostly linear functions. The area resistances ($\Omega^{-1}$ $cm^{2-}$) and proton conductivities ($\Omega^{-1}$ $cm^{-1}$) were calculated (Equation (8)) from the slopes of the linear regions on these dependences. Based on the values of proton conductivities, the membranes can be arranged in the following series: p-PVA/tungsto-phosphate ($4.8·10^{-2}$) > bipolar Selemion HSF ($4.0·10^{-2}$) > Nafion 117 ($2.6·10^{-2}$) > partially phosphorylated PVA ($1.8·10^{-2}$ $\Omega^{-1}$ $cm^{-1}$ [6]). It can be seen that the attachment of the lacunary tungsto-phosphoric acid to the partially phosphorylated PVA backbone facilitates the proton transfer. The increase in proton conductivity is quite significant and amounts to 2.7-fold in comparison with the partially phosphorylated PVA membrane. In addition, the synthesized membrane has a comparable or higher proton conductivity as compared to the studied commercially available membranes.

### 3.5. Testing of the Membrane in a BioGenerator $Fe^{3+}/H_2$ Electrochemical Cell

The results of the membrane testing in $Fe^{3+}/H_2$ fuel cell with microbiological regeneration of ferric ions are presented in Figure 8. The figure compares the current-voltage behavior of the electrochemical cell at 40 °C using the fabricated membrane and Selemion HSF. As can be seen in the figure, the power density of the fuel cell is almost equal in both membranes at low current densities. However, above 0.1 $A·cm^{-2}$, the difference in performance becomes more significant and continues to increase as the current density increases. In the case of the p-PVA/tungsto-phosphate membrane, the maximum power density of 0.28 $W·cm^{-2}$ was reached at about 0.79 $A·cm^{-2}$, whereas the maximum power density

of only 0.18 W·cm$^{-2}$ was obtained with Selemion HSF membrane at 0.60 A·cm$^{-2}$. Thus, the beneficial effect of the application of the developed membrane in the BioGenerator is obvious.
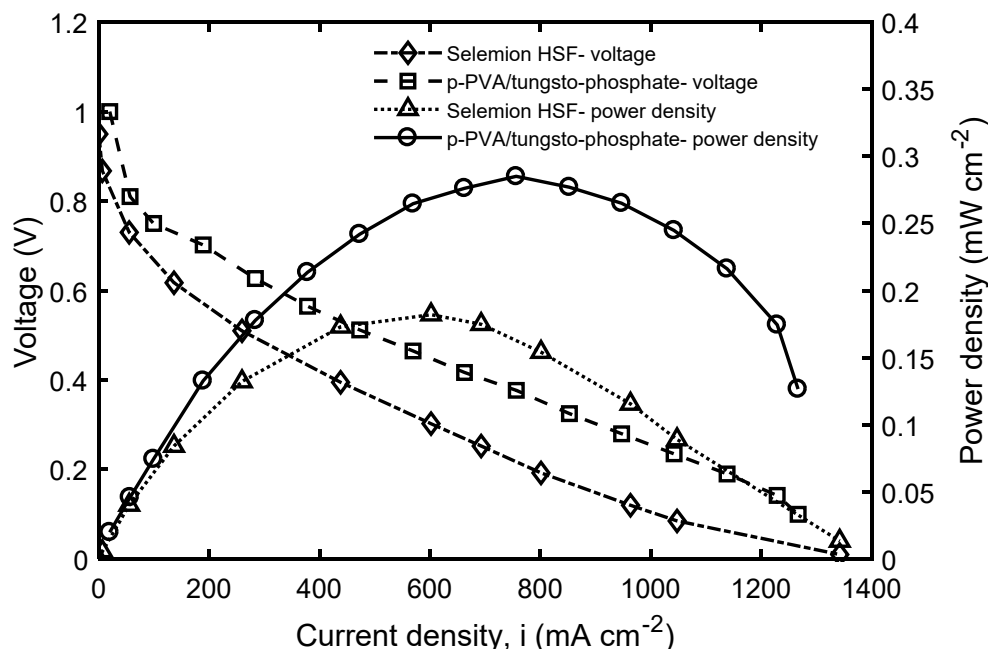


**Figure 8.** The performance of Fe$^{3+}$/H$_2$ electrochemical cell with the p-PVA/tungsto-phosphate and Selemion HSF membranes.

## 4. Conclusions

1.  The synthesis of a hybrid p-PVA (partially phosphorylated polyvinyl alcohol)/tungsto-phosphate membrane was performed via a casting technique followed by a thermal treatment to achieve a desired extent of cross-linking.
2.  The XPS study of the obtained membrane revealed that tungsten present, therein, was predominantly in the oxidation states of W$^{6+}$ and W$^{5+}$. Presumably, such behavior can be explained by the partial reduction of tungsten oxometallate ions by polymer matrix during synthesis.
3.  Based on the thorough analysis of the FTIR spectra, the two possible reactions leading to the covalent bonding of tungsto-phosphate anions to the polymer matrix were suggested. Supposedly, a moderately large number of C=C double bonds in the polymer matrix can result in the formation of epoxide cycles (under the conditions of synthesis), which, in turn, are prone to reaction with tungsto-phosphate anions. Another path is via the reaction between tri-vacant [PW$_9$O$_{34}$]$^{9-}$ anion and the accessible -PO(OH)$_2$ functional groups.
4.  The bonding of lacunary tungsto-phosphate anions to the p-PVA matrix greatly improves the proton transfer within it and, thereby, increases conductivity of the membrane. This allowed for a 2.7-fold increase in the proton conductivity in comparison with the original p-PVA membrane. In addition, the developed membrane exhibited comparable or better proton conductivity, as compared to the studied commercial membranes.
5.  The testing of the hybrid p-PVA/tungsto-phosphoric acid and commercial Selemion HSF membranes in the Fe$^{3+}$/H$_2$ electrochemical cell showed that in the case of hybrid membrane, the maximum power density of 0.28 W·cm$^{-2}$ was achieved at the current density of 0.79 A·cm$^{-2}$, unlike the Selemion HSF, which achieved the maximum power density of only 0.18 W·cm$^{-2}$ at 0.60 A·cm$^{-2}$. The above results are a good indication of a potential application of this type of membrane in the BioGenerator system.

## References

1. Schröder, U.F.; Harnisch, L.T. Angenent, Microbial electrochemistry and technology: Terminology and classification. *Energy Environ. Sci.* **2015**, *8*, 513–519. [CrossRef]
2. Lovley, D.R. Powering microbes with electricity: Direct electron transfer from electrodes to microbes. *Environ. Microbiol. Rep.* **2011**, *3*, 27–35. [CrossRef] [PubMed]
3. Logan, B.E. Scaling up microbial fuel cells and other bioelectrochemical systems. *Appl. Microbiol. Biotechnol.* **2010**, *85*, 1665–1671. [CrossRef]
4. Nicola, S. Merkel's other crisis spurs German quest for energy holy grail. *Bloomberg*. 26 August 2012. Available online: https://www.bloomberg.com/news/articles/2012-08-26/merkel-s-other-crisis-spurs-german-quest-for-energy-holy-grail (accessed on 5 July 2019).
5. Karamanev, D.; Pupkevich, V.; Hojjati, H. Bio-Fuel Cell System. US Patent 8455144, 4 June 2013. Available online: https://patents.justia.com/patent/8455144 (accessed on 5 July 2019).
6. Karamanev, D.; Pupkevich, V.; Penev, K.; Glibin, V.; Gohil, J.; Vajihinejad, V. Biological conversion of hydrogen energy to electricity for energy storage. *Energy* **2017**, *129*, 237–245. [CrossRef]
7. Pupkevich, V.; Glibin, V.; Karamanev, D. The effect of ferric ions on the conductivity of various types of polymer cation exchange membranes. *J. Solid State Electrochem.* **2007**, *11*, 1429–1434. [CrossRef]
8. Glibin, V.; Pupkevich, V.; Svirko, L.; Karamanev, D. Preparation and characterization of hybrid Nafion/silica and Nafion/silica/PTA membranes for redox flow batteries. *J. New. Mat. Electrochem. Syst.* **2009**, *12*, 195–199.
9. Balgobin, R.; Garcia, B.; Karamanev, D.; Glibin, V. Preparation and proton conductivity of composite $SiO_2$/Poly(2-hydroxyethyl methacrylate) gel membranes. *Solid State Ionics* **2010**, *181*, 1403–1407. [CrossRef]
10. Pupkevich, V.; Glibin, V.; Karamanev, D. Phosphorylated polyvinyl alcohol membranes for redox $Fe^{3+}$/$H_2$ fuel cells. *J. Power Sources* **2013**, *228*, 300–307. [CrossRef]
11. Gohil, J.M.; Karamanev, D. Novel pore-filled polyelectrolyte composite membranes for cathodic microbial fuel cell application. *J. Power Sources* **2013**, *243*, 603–610. [CrossRef]
12. Binsu, V.V.; Nagarale, R.K.; Shahi, V.K. Phosphonic acid functionalized aminopropyl triethoxysilane-PVA composite material: Organic-inorganic hybrid proton-exchange membranes in aqueous media. *J. Mater. Chem.* **2005**, *15*, 4823–4831. [CrossRef]
13. Hiroshi, A.; Masao, I.; Masaru, I.; Hiroyuki, O. Sulphonic Acid Group-Containing Polyvinyl Alcohol, Solid Polymer Electrolyte, Composite Polymer Membrane, Method for Producing the Same and Electrode. US Patent 6523699, 25 February 2003. Available online: https://patents.google.com/patent/US6523699B1/en (accessed on 5 July 2019).
14. Boroglu, M.S.; Cavus, S.; Boz, I.; Ata, A. Synthesis and characterization of poly(vinyl alcohol) proton exchange membranes modified with 4,4-diaminophenylether-2,2 disulphonic acid. *Express Polym. Lett.* **2011**, *5*, 470–478. [CrossRef]
15. Qinbai, F.; Hamid, H. High Temperature Composite Proton Exchange Membrane. US Patent 7115333, 10 March 2006.
16. Jiang, Z.; Zheng, X.; Wu, H.; Pan, F. Proton conducting membranes prepared by incorporation of organophosphorus acids into alcohol barrier polymers for direct methanol fuel cells. *J. Power Sources* **2008**, *185*, 85–94. [CrossRef]
17. Şahin, A.; Ar, I. Synthesis, characterization and fuel cell performance tests of boric acid and boron phosphate doped, sulphonated and phosphonated poly(vinyl alcohol) based composite membranes. *J. Power Sources* **2015**, *288*, 426–433. [CrossRef]
18. Kim, Y.S.; Wang, F.; Hickner, M.; Zawodzinski, T.A.; McGrath, J.E. Fabrication and characterization of heteropolyacid ($H_3PW_{12}O_{40}$)/directly polymerized sulfonated poly(arylene ether sulfone) copolymer composite membranes for higher temperature fuel cell applications. *J. Membr. Sci.* **2003**, *212*, 263–282. [CrossRef]
19. Li, L.; Xu, L.; Wang, Y. Novel proton conducting composite membranes for direct methanol fuel cell. *Mater. Lett.* **2003**, *57*, 1406–1410. [CrossRef]
20. Honma, I.; Nomura, S.; Nakajima, H. Protonic conducting organic/inorganic nanocomposites for polymer electrolyte membrane. *J. Membr. Sci.* **2001**, *185*, 83–94. [CrossRef]
21. Ponce, M.L.; de Prado, L.A.S.A.; Silva, V.; Nunes, S.P. Membranes for direct methanol fuel cell based on modified heteropolyacids. *Desalination* **2004**, *162*, 383–391. [CrossRef]
22. Ponce, M.L. Organic-Inorganic Hybrid Membranes with Heteropolyacids for DMFC Applications. Ph.D. Thesis, University of Hamburg, Hamburg, Germany, 2004.

23. Vernon, D.R.; Meng, F.; Dec, S.F.; Williams, D.L.; Turner, J.A.; Herring, A.M. Synthesis, characterization, and conductivity measurements of hybrid membranes containing a mono-lacunary heteropolyacid for PEM fuel cell applications. *J. Power Sources* **2005**, *139*, 141–151. [CrossRef]

24. Kourasi, M.; Wills, R.G.A.; Shah, A.A.; Walsh, F.C. Heteropolyacids for fuel cells applications. *Electrochim. Acta* **2014**, *127*, 454–466. [CrossRef]

25. Pope, M.T. Isopoly and Heteropolyanions. In *Comprehensive Coordination Chemistry*; Wilkinson, G.W., Gillard, R.D., McCleverty, J.A., Eds.; Pergamon Press: Oxford, UK, 1987.

26. Zhu, Z.; Tain, R.; Rhodes, C. A study of the decomposition behavior of 12-tungstophosphate heteropolyacid in solution. *Can. J. Chem.* **2003**, *81*, 1044–1050. [CrossRef]

27. Judenstein, P. Synthesis and properties of polyoxometallates based inorganic-organic polymers. *Chem. Mater.* **1992**, *4*, 4–7. [CrossRef]

28. Mayer, C.R.; Thouvenot, R. Organophosphoryl derivatives of trivacant tungstophosphates of general formula $\alpha$-A-$[PW_9O_{34}(RPO)_2]^{5-}$: Synthesis and structure determination by multinuclear magnetic resonance spectroscopy ($^{31}P$, $^{183}W$). *J. Chem. Soc. Dalton Trans.* **1998**, *1*, 7–13. [CrossRef]

29. Pupkevich, V. Scale-Up and Study of the BioGenerator. Ph.D. Thesis, The University of Western Ontario, London, ON, Canada, 2014.

30. Tretinnikov, O.N.; Sushko, N.I. Formation of linear polyenes in thermal dehydration of polyvinyl alcohol catalyzed by phospho-tungstic acid. *J. Appl. Spectrosc.* **2015**, *81*, 1044–1047. [CrossRef]

31. Pruethiarenum, K.; Isobe, T.; Matsushita, S.; Ye, J.; Nakajima, A. Comparative study of photoinduced wettability conversion between $[PW_{12}O_{40}]^{3-}$/brookite and $[SiW_{12}O_{40}]^{4-}$/brookite hybrid films, Mater. *Chem. Phys.* **2014**, *144*, 327–334.

32. Hsu, Y.-G.; Lin, K.-H.; Hung, L.-M.; Hua, C.-H.; Hsieh, C.-H. Properties of PVA-PSA hybrid materials prepared through the incorporation of polysilicic acid (PSA) into polyvinyl alcohol. *J. Polym. Res.* **2001**, *8*, 125–132. [CrossRef]

33. Hellal, A.; Chafaa, S.; Chafai, N. Synthesis, characterization and computational studies of three $\alpha$-amino-phosphonic acids derivatives from meta, ortho and para aminophenols. *J. Mol. Struct.* **2016**, *1103*, 110–124. [CrossRef]

34. Thermo Scientific. *Knowledge Base: Infrared Spectral Interpretation*; Fisher Scientific Inc.: Waltham, MA, USA, 2009. Available online: http://www.thermo.com/spectroscopy (accessed on 5 July 2019).

35. Mioč, U.B.; Todorovich, M.R.; Davidović, M.; Colomban, P.; Holclajtner-Antunović, I. Heteropoly compounds-from proton conductors to biomedical agents. *Solid State Ionics* **2005**, *176*, 3005–3017. [CrossRef]